Hydrophilic surface morphology for intricate conductive coatings

Taylor Stark^a, Stanislav Sikulskyi^a, Rishikesh Srinivasaraghavan Govindarajan^a, Daewon Kim*^a Dept. of Aerospace Engineering, Embry-Riddle Aeronautical University, 1 Aerospace Blvd, Daytona Beach, FL, USA 32114

ABSTRACT

Conductive surfaces and patterns are at the forefront of electronics research with a need to go smaller and create more intricate electronic designs and devices while still maintaining easy manufacturability. This paper investigates an approach of patterning conductive traces for microsize electrically driven devices with the focus on enabling and patterning complicated geometries. The approach includes the design and fabrication of hydrophilic microstructures along the channels with hydrophobic borders on devices' surfaces. The channels are connected to larger electrodes outside the device. When a conductive solution is applied to the outside electrode area, hydrophilic morphologies stimulate the solution to feed along the channels and fill the predesigned patterns. Therefore, the major objective of this study is to explore different designs of microstructures to increase surface hydrophilicity for liquid electrode patterning for variously oriented surfaces. Due to numerous physical forces, material domains, and interactions involved, experimental approach is selected to study the method of surface electrode micropatterning through wetting. Microstructured surfaces are fabricated using the two-photon polymerization 3D printing technique due to its superior resolution. Analysis of various morphologies is completed, a microsize electromechanical device with selected hydrophilic morphologies is fabricated, patterned with liquid electrode, and tested. The findings in this paper further the development of electrode patterning and help determine which hydrophilic microstructures show superior patterning ability along horizontal and vertical vectors.

Keywords: two-photon polymerization, hydrophilic, hydrophobic, electrode patterning, additive manufacturing, actuators, printing, microstructures

1. INTRODUCTION

Numerous electrical technologies rely on translating the signals and powering devices through electrodes constructed of electrically conductive materials. Within the field of smart materials, electrical type of stimuli remains the most common type due to its reliability, low interference, and relative simplicity. Particularly, numerous microelectromechanical systems (MEMS) and robotics heavily rely on small size patterns of conductive traces. While a great progress was accomplished in micropatterning for electrical systems for last several decades, some challenges intrinsic to novel MEMS are yet to be addressed.^{1, 2, 3}. Firstly, the dynamically growing field of MEMS and small robotics can benefit from a manufacturing method of producing electrodes and conductive traces that can be effectively adapted to various designs⁴. Secondly, a method that is capable of micropatterning electrodes on top of complex geometries is essential for many biomimetic or topologically optimized designs of MEMS and small robotics⁵. One solution for these requirements can be application of additive manufacturing (AM) to directly fabricate electrodes on various surfaces. While this allows various electrode designs to be fabricated, performing that on complex geometries requires sophisticated 3D printers with multiaxial coordinate stages, so called conformal 3D printing^{6, 7}. This paper presents an alternative approach of creating complex and conformal electrode patterns in which AM is utilized to fabricate the main part, e.g., MEMS or small-scale robot body, with auxiliary microstructures on its surface (Figure 1a). These microstructures are then used to control surface wettability and drive the liquid electrode, e.g., liquid metal or conductive polymer solution, into a desired electrode design (Figure 1b-1c). The challenges of this approach are an appropriate AM technique, which is capable of producing both the main part of the MEMS and the auxiliary microstructures, as well as the design of the microstructures that properly alter surface wettability in a local fashion but do not compromise MEMS's functionality.

^{*} kimd3c@erau.edu; Phone 1-386-226-7262; ERAU SMART Lab

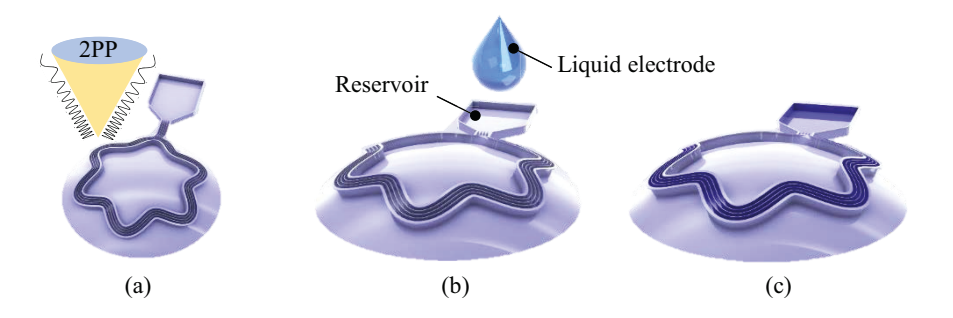


Figure 1. Schematics of the complex and conformal electrode micropatterning consisted of (a) additive manufacturing of a functional part with designed microchannels and microstructures through two-photon polymerization (2PP), (b) supplying liquid electrode into reservoir, and (c) electrode material transfer by the capillary action with the following option curing.

For the AM technique, two-photon polymerization (2PP) AM method was selected for its superior spatial resolution than other 3D additive manufacturing techniques while being extremely versatile and precise with resolutions down to sub millimeter scales^{8,9}. The 2PP process uses a femtosecond laser that emits 780nm wavelength light that is focused using a lens where the focal point of the light is converted to the UV spectrum, where polymerization of the photoresists occurs. This is able to get the printing voxel considerably smaller than other 3D printing techniques, such as stereolithography (SLA) that is able to get small features but not near the capabilities and submicron feature sizes that 2PP can give^{9, 10}. To create small open microchannels with microstructures inside, a technique of printing near sub micrometer with high precision was needed.

For the microstructures, walls with hydrophobic sleeves can serve to build a pattern of open microchannels and an inlet pool. By dropping liquid electrode material in the pool, channels can be filled with the conductive material through capillary action and form conductive traces and electrodes. It is advantageous for many applications to have flat and uniform electrodes, which can be achieved with rectangular channel cross-section. While wettability is already a non-trivial phenomenon that depends on the balance of surface tension, viscosity, and gravity, rectangular shape further complicates the process¹¹. Various modes of capillary flow are possible depending on the height to width ratio, $\lambda = H/W$, of the rectangular channel cross-section¹². Particularly, the main parameter to look after is the critical aspect ratio, λ_c , of the channel that is written with an equilibrium contact angle θ_o , as in Equation (1). When the actual channel aspect ratio is below the critical value, liquid flow in the corners of the channel wets the entire vertical wall length, so called pinned state (Figure 2). In contrast, pinned case with $\lambda > \lambda_c$ has corner flow that does not wet the entire vertical wall height. Besides that, liquid flow in rectangular channels with low aspect ratio, λ , are characterized by a larger transition zone between the meniscus and corner flow leaving larger surface area at the tip on the flow uncovered with the fluid. For the electrode coating and micropatterning, above two factors are important as they control where the liquid electrode is deposited during the coating process. Thus, the channel geometry needs to be thought through for both electrode filling and application purposes. Lastly, evaporation plays an important role in wetting microsize open channels limiting the maximum distance that the liquid can travel in the open channel 12, 13. Thus, evaporation effect needs to be considered if a correct liquid flow is desired.

$$\lambda_c = (1 - \sin\theta_o) / 2\cos\theta_o \tag{1}$$

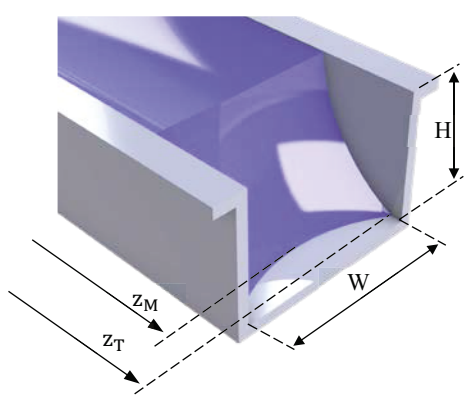


Figure 2. Simplified free-surface morphology of a liquid electrode in the rectangular open channel with high height-to-width ratio.

To increase the capillary action of the liquid conductive material and enable coating larger electrodes and conductive traces, additional microstructures can be added inside the channel. By increasing the surface area of the surface that gets in touch with the fluid, hydrophilic behavior of the surface can be enhanced. The geometry of the microstructures should not form reentry structures with hydrophobic behavior and should tend to be as continuous nature as possible to enhance capillary effect without breaches. An example of such shape can be continuous ribs as shown in Figure 3a, which would effectively increase the contact area and ensure the contact with fluid along the whole channel. The contribution of such ribs to the fluid capillary action inside the channel is equivalent to decreasing the width of the channel. However, some MEMS designs that utilize micropatterned electrodes might require sufficient compliance to function and can be stiffened by the continuous ribs inside the channels. Thus, for such applications, it might be useful to have microstructure that provides some capillary action improvement over the empty rectangular microchannel while does not considerably affect its stiffness. By discretizing the ribs into smaller segments and sharpening their edges to reduce the back pressure, a diamond shape microstructure can be obtained as shown in Figure 3b. The step of the diamond microstructures along the channel should be selected such that the contact between the fluid and following microstructures occurs. Thus, step should be equal or small than the distance between the fluid corner flow and meniscus position, $z_M - z_T$, which is a dynamically changing and increasing value as the liquid transfers through the channel¹³.

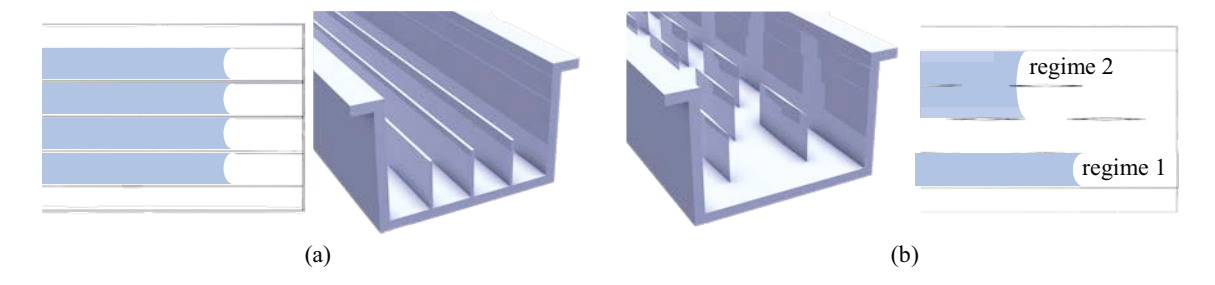


Figure 3. (a) Continuous ribs and (b) diamond shape microstructures added to the rectangular open channel to increase capillary action.

2. METHODS

Design of the open channels and microstructures was created in CATIA and processed in DeScribe software (Nanowrite) for dip-in laser lithography (DiLL) using two-photon polymerization process in a Nanoscribe Photonic Professional GT2 system (Nanoscribe, Eggenstein-Leopoldshafen, Germany). A 25x 0.8 numerical aperture lens is used with IP-S photoresist (Nanoscribe) on indium tin oxide (ITO) coated glass substrates. The substrates were cleaned in a deionized water bath for 2-5 minutes, then in 99.5% acetone bath for 1-3 minutes, and finally into a 99.9+% isopropanol (IPA) bath for 2-8 minutes. All cleaning baths were performed with heated sonication. Afterwards the substrates were blow-dried and activated with oxygen plasma for 30 seconds using a Plasma Etch PE-50HF system.

Table 1. Parameters used for 2PP printing on ITO glass with 25x objective.

Resin	IP-S
Slicing, µm	1
Hatching, μm	0.5
Base Count	6
Core Power, mW	50
Base Power, mW	40
Core Writing Speed, µm/s	100,000
Base Writing Speed, μm/s	100,000

Once the cleaning and activation of the substrates were completed, IP-S resin was placed in the center of the substrate and printed with the parameters found in Table 1. After printing, the printed part was developed in propylene glycol monomethyl ether acetate (PGMEA) for 20 minutes, IPA for 5 minutes, and then blow-dried. The final printed part after development and drying can be seen in Figure 4, displaying the two different micropatterns (a) and (c) along with a control (b).

Testing of the open channels utilized 2-5 mL of PEDOT:PSS solution inside of a 10 mL syringe (Becton, Dickinson and Company) with a 32-gauge Luer-Lok™ tip installed. The syringe was primed with a small drop of PEDOT:PSS solution, seen in Figure 5, and was promptly placed onto the electrode pad area. This was repeated for all fabricated channels with expulsion of PEDOT:PSS material from the syringe between sample testing and before priming of the drop. This was to maintain the consistency of the solution since over time the water dries out of the PEDOT:PSS solution in the tip causing either excess PEDOT:PSS material in the drop or no material to be dispensed.



Figure 4. IP-S fabricated open microchannels with (a) micro diamonds, (b) control, and (c) micro ribs.



Figure 5. PEDOT:PSS primed at tip of needle for placement on pad areas.

Once testing was completed, the printed microchannels were cleaned with deionized water, then with IPA, and dried. The experiment was repeated multiple times per printed samples.

3. ANALYSIS OF GEOMETRY

To have microchannels with a high likelihood of propagation of the liquid electrodes, certain design parameters had to be taken into consideration. Design of the channels required an understanding of material surface properties and contact interaction of the propagating liquid with the channels material.

3.1 Channel shape selection

As discussed in the Introduction, two states of corner flow is possible inside a rectangular channel depending on the geometrical aspect ratio of the channel and the critical aspect ratio (Equation (1)). The contact angle of the utilized PEDOT:PSS solution composition on cured IP-S surface as measured to be just below 45°, which corresponds to the critical aspect ratio for the selected material of λ_c =0.207. To ensure a proper transfer of liquid electrode through the channel in this study, height to width ratio of 0.7 was selected for the microchannel cross-section (119 µm height, 170 µm width). The selected value is higher than the theoretical maximum value of 0.5 for the critical aspect ratio to ensure the flow state will note change even after the 3D printed IP-S surface is treated with oxygen plasma before applying PEDOT:PSS solution.

3.2 Ribs and diamonds shape selection

Introducing ribs microstructures into the rectangular channel is equivalent to creating multiple channels with higher aspect ratio, from 0.7 to 3 for the selected channel and ribs sizing (Figure 3a). Diamond microstructures have a similar effect but their step along the channel needs to be sufficient to provide a seamless contact between the fluid and the microstructures. While the free-surface morphology changes as the fluid propagates through the channel, the channels with high aspect ratio of 1.5-3, depending on the flow regime (Figure 3b), lead to a relatively small difference between the meniscus and corner flow edges, $z_M - z_c$. Thus, a moderate spacing between the diamond shapes equal to half of the diamond shape length was utilized for the initial electrode coating tests.

4. RESULTS

Experimental tests can be seen in Figure 6 with the same orientation as displayed in Figure 4. The tests show that the rib design, seen in Figure 6c, performed the best with the diamond design, seen in Figure 6a, exhibiting lower hydrophilicity than the control, seen in Figure 6b. In the 5 mm open microchannels, the PEDOT:PSS was able to travel an average of 8% up the diamond microstructure channels, 22% up the control design channels, and 95% up the rib microstructure channels. The diamond structures appeared to act more hydrophobic in the channels, purportedly from either contaminants stuck inside, evaporation on the surface of the PEDOT:PSS causing thickened material to block propagation, pillowing effect that is distinctively from the 2PP process in block stitching during printing, or any combination of these.

It was noted that block splitting of the printed part distinctively had some effect on the propagation of PEDOT:PSS through the channels as is evident by Figure 7, where the rib design channels specifically propagate further in some regions than in others and are stopped at the block stitching zones. This is most likely due to a pillowing effect that can cause a ridge or pillow near the block stitched regions due to extra free radicals from the overlap of block regions and partially polymerized resin.

Printed parts, once cleaned, were activated with oxygen plasma for 20 seconds to determine if

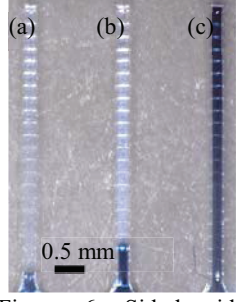


Figure 6. Side-by-side tests of open hydrophilic microchannels with (a) diamond, (b) control, and (c) rib designs.

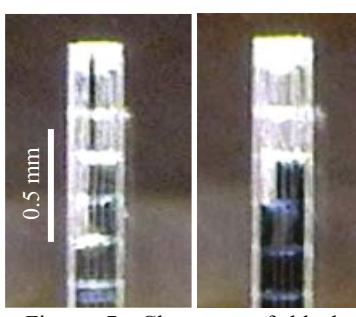


Figure 7. Close up of block splitting on the rib design microchannel with PEDOT:PSS unevenly propagating.

oxygen plasma could increase the hydrophilicity of the channels and overcome the regions stopping flow, seen in Figure 7. Activating the channels with plasma allowed all channels to propagate PEDOT:PSS from the pads to the far end, proving that plasma activation is able to overcome small issues in the micro parts when trying to make surfaces hydrophilic in nature.

Profilometry data was gathered to determine flatness of the walls as well as the details inside the channels and print quality. Figure 8 shows the top views and cross-sectional views of the three different micro channel structures. It can be seen that the channels were well developed and show little to no deformities in the structure as well as very flat vertical and horizontal surfaces as was designed.

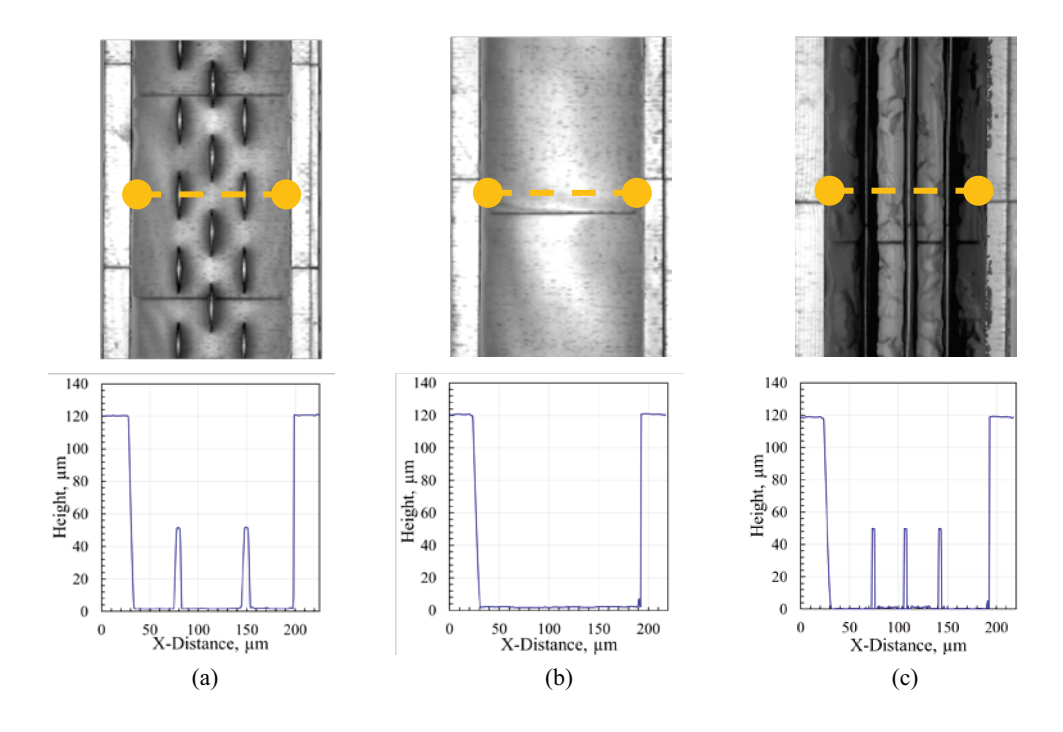


Figure 8. Profilometry images and cross sections of (a) diamond channel, (b) control channel, and (c) rib channel.

5. APPLICATION

An application where microchannels could be used and implemented into a MEMS device like a corneal sensor⁵ was fabricated and implemented with microchannels using 2PP process with the final product seen in Figure 9a. After testing with PEDOT:PSS, seen in Figure 9b, it was evident that the channels were being blocked. To help propagate the electrode through the blockages, the part was cleaned, subjected to oxygen plasma, and tested again, seen in Figure 9c. After plasma activation, the electrode channels were able to be fully filled with PEDOT:PSS.

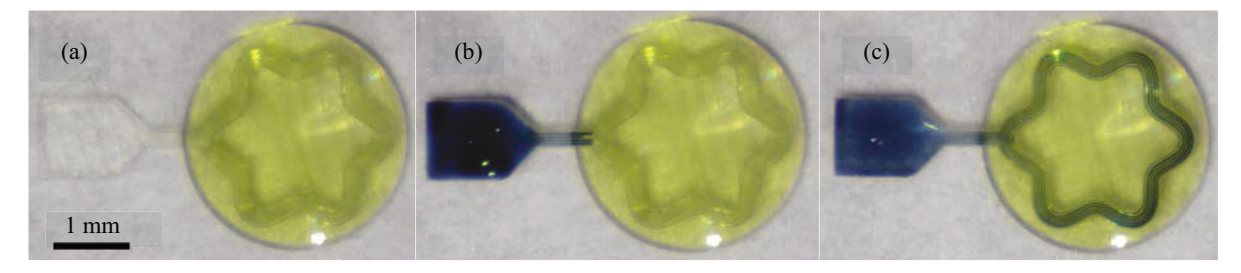


Figure 9. Star design, based off of corneal sensor⁵, printed with IP-S resin. (a) Original print. (b) Tested print. (c) Tested print after plasma activation.

6. CONCLUSION

Simple microstructure additions were added to open electrode channels and determined that of the two designs tested against the control, the diamond structure was more hydrophobic than the control with the rib structure being the most effective. Though rib structure additions to the microchannels is able to propagate electrodes better than empty channels, the propagation of the liquid electrodes is most prominent when the surface has been activated by oxygen plasma. It is for this reason that surface activation with oxygen plasma is recommended as an additional step for liquid electrode propagation through open microchannels.

ACKNOWLEDGMENT

This material is based upon work supported by the National Science Foundation under Grant No. 2229155. The opinions, findings, and conclusions, or recommendations expressed are those of the author(s) and do not necessarily reflect the views of the National Science Foundation.

REFERENCES

- [1] Hines, L., et al., "Soft Actuators for Small-Scale Robotics," Advanced Materials, 29(13), p. 1603483, (2017).
- [2] Yang, J.C., et al., "Electronic Skin: Recent Progress and Future Prospects for Skin-Attachable Devices for Health Monitoring, Robotics, and Prosthetics," Advanced Materials, 31(48), p. 1904765, (2019).
- [3] Srinivasaraghavan Govindarajan, R., Stark, T., Sikulskyi, S., Madiyar, F., and Kim, D., "Piezoelectric strain sensor through reverse replication based on two-photon polymerization," In Proc. of SPIE Vol, pp. 1204611-1, (2022).
- [4] Rehmani, M.A.A., et al., "Laser ablation assisted micropattern screen printed transduction electrodes for sensing applications," Scientific Reports, 12(1): p. 6928, (2022).
- [5] Kim, K., et al., "All-printed stretchable corneal sensor on soft contact lenses for noninvasive and painless ocular electrodiagnosis," Nature Communications, 12(1): p. 1544, (2021).
- [6] Lu B H, Lan H B, and Liu H Z., "Additive manufacturing frontier: 3D printing electronics," Opto-Electron Advances, 1 (1), 170004, (2018).
- [7] Emon, O.F., et al., "Conformal 3D printing of a polymeric tactile sensor," Additive Manufacturing Letters, 2, p. 100027, (2022).
- [8] Bunea, A.-I., del Castillo Iniesta, N., Droumpali, A., Wetzel, A. E., Engay, E., and Taboryski, R., "Micro 3D Printing by Two-Photon Polymerization: Configurations and Parameters for the Nanoscribe System," Micro, 1(2), 164–180, (2021).
- [9] Faraji Rad, Z., Prewett, P.D. and Davies, G.J., "High-resolution two-photon polymerization: the most versatile technique for the fabrication of microneedle arrays," Microsyst Nanoeng, 7, 71, (2021).
- [10] Maruo, S., and Ikuta, K., "Submicron stereolithography for the production of freely movable mechanisms by using single-photon polymerization," Sensors and Actuators A: Physical, 100(1), 70–76, (2002).
- [11] Seemann, R., et al., "Wetting morphologies at microstructured surfaces," Proceedings of the National Academy of Sciences, 102(6), p. 1848-1852, (2005).
- [12] Kolliopoulos, P. and S. Kumar, "Capillary flow of liquids in open microchannels: overview and recent advances," npj Microgravity, 7(1), p. 51., (2021).
- [13] Kolliopoulos, P., et al., "Capillary flow of evaporating liquid solutions in open rectangular microchannels," Journal of Fluid Mechanics, 938, p. A22, (2022).